Neoplasma 2023; 70(5): 621–632

doi:10.4149/neo_2023_230719N376

ΔNp63 is regulated by insulin/IGF-1 signaling in normal basal/progenitor mammary cells and in luminal-type breast cancer cells

Michaela STENCKOVA[1,2], Yajing LIU[3], Marta NEKULOVA[1], Jitka HOLCAKOVA[1], Zuzana POKORNA[1], Rudolf NENUTIL[1], Alastair M. THOMPSON[4], Borivoj VOJTESEK[1,*], Philip John COATES[1,*]

[1]Research Centre for Applied Molecular Oncology, Masaryk Memorial Cancer Institute, Brno, Czech Republic; [2]Department of Experimental Biology, Faculty of Science, Masaryk University, Brno, Czech Republic; [3]North Campus Research Complex, University of Michigan, Ann Arbor, Michigan, United States; [4]Division of Surgical Oncology, Lester and Sue Smith Breast Center, Dan L Duncan Comprehensive Cancer Center, Baylor College of Medicine, Houston, Texas, United States

**Correspondence: vojtesek@mou.cz; philip.coates@mou.cz*

Received July 19, 2023 / Accepted October 3, 2023

Breast cancers are a heterogeneous group of tumors classified according to their histological growth patterns and receptor expression characteristics. Intratumor heterogeneity also exists, with subpopulations of cells with different phenotypes found in individual cancers, including cells with stem or progenitor cell properties. At least two types of breast cancer stem cells (CSCs) exist, the epithelial and the basal/mesenchymal subtypes, although how these phenotypes are controlled is unknown. ΔNp63 is a basal cell marker and regulator of stem/progenitor cell activities in the normal mammary gland and is expressed in the basal-like CSC subpopulation in some estrogen receptor-positive (ER^+) and/or human epidermal growth factor receptor 2-positive ($HER2^+$) breast adenocarcinomas. Whilst p63 is known to directly impart CSC properties in luminal breast cancer cells, how p63 is regulated and induced in these cells is unknown. We initially confirmed the existence of a small subpopulation of $\Delta Np63^+$ cells in lymph node metastases of ER^+ human ductal adenocarcinomas, indicating together with previous reports that $\Delta Np63^+$ tumor cells are present in approximately 40% of these metastases. Notably, $\Delta Np63^+$ cells show a preferential location at the edge of tumor areas, suggesting possible regulation of ΔNp63 by the tumor microenvironment. Subsequently, we showed that the high levels of ΔNp63 in basal non-transformed MCF-10A mammary epithelial cells rely on insulin in their culture medium, whilst ΔNp63 levels are increased in MCF-7 ER^+ luminal-type breast cancer cells treated with insulin or insulin-like growth factor 1 (IGF-1). Mechanistically, small molecule inhibitors and siRNA gene knockdown demonstrated that induction of ΔNp63 by IGF-1 requires PI3K, ERK1/2, and p38 MAPK activation, and acts through FOXO transcriptional inactivation. We also show that metformin inhibits ΔNp63 induction. These data reveal an IGF-mediated mechanism to control basal-type breast CSCs, with therapeutic implications to modify intratumor breast cancer cell heterogeneity and plasticity.

Key words: breast cancer stem cells; ΔNp63; insulin; IGF-1; tumor microenvironment

ΔNp63 is an oncogenic isoform of the p53-related transcription factor p63 and is essential for stem cell activities in many epithelial tissues [1, 2]. In particular, ΔNp63 is a marker of basal/myoepithelial cells in the mammary gland [3], where mammary stem/progenitor cells reside [4]. Expression of ΔNp63 in luminal cells is sufficient to induce a basal cell phenotype [5], and ΔNp63 promotes stem cell activities during mammary gland development and in tumors [6–8]. Within breast cancers, high levels of ΔNp63 are characteristic for the basal subtype of triple negative cancers [7–10], where these cancers typically contain 20–80% of $p63^+$ cells [11, 12], and ΔNp63 acts to aid survival, proliferation, and migration, activate epidermal growth factor receptor (EGFR) signaling, and recruit myeloid-derived suppressor cells to the tumor microenvironment [7, 13–16]. ΔNp63 is also sometimes found in a small population of cancer cells in human estrogen receptor-positive (ER^+) or human epidermal growth factor receptor 2-positive ($HER2^+$) luminal-type breast cancers [17, 18]. The phenotype of $\Delta Np63^+$ cells in luminal breast cancer is that of the "basal-like" or "mesenchymal-like" cancer stem cell (CSC) subtype, characterized by expression of CD44 or CD271 and lack of epithelial markers [17–19], contrasting with "epithelial-like" breast CSCs that were described as $CD44^-/CD271^-$ and $ALDH^+$/milk mucin$^+$ [17, 19]. These

two different types of CSC are also reported to show distinct locations, with epithelial CSCs seen mainly in the tumor body and basal CSCs at the tumor periphery [17–19].

Whilst previous studies have shown the presence of ΔNp63 in luminal ER$^+$ breast cancers, and have demonstrated that ΔNp63 directly induces a CSC phenotype in these cells [8, 20, 21] (reviewed in [22]), how ΔNp63 is regulated in luminal ER$^+$ tumor cells is unknown. Based on their location and the evidence that CSCs depend on their microenvironment (the CSC niche) [23–25], we hypothesized that stromal-derived factors may be responsible for inducing ΔNp63 in cells at the tumor/stroma interface. We identified insulin/insulin-like growth factor 1 (IGF-1) as a major inducer of ΔNp63 in both non-transformed mammary basal progenitor cells (MCF-10A) and ER$^+$/PR$^+$/HER2$^-$ luminal-A breast cancer cells (MCF-7). Small molecule inhibitors and siRNAs were used to delineate the regulatory pathway for ΔNp63 induction in luminal breast cancer cells, involving extracellular signal-regulated kinase (ERK)/mitogen-activated protein kinase (MAPK) activity and forkhead box O (FOXO) signaling. These data implicate insulin/IGF-1 signaling as a modulator of breast cancer cell phenotypes with implications for therapeutic intervention.

Patients and methods

Human breast cancer samples. Formalin-fixed, paraffin-embedded blocks of axillary lymph nodes containing metastatic deposits of ER$^+$ ductal breast carcinoma from 28 patients who were diagnosed and underwent surgery at the Masaryk Memorial Cancer Institute in Brno were retrieved. The use of lymph node metastases avoids the problem of identifying non-malignant ΔNp63$^+$ myoepithelial cells that might be present surrounding the tumor in primary cancers-metastatic tumor deposits contain only the malignant cell population and are devoid of contaminating normal myoepithelium. Permission for the use of anonymized excess human tissues was approved by the Biobank of Clinical Samples at the Masaryk Memorial Cancer Institute following a local ethical committee review (NS/10357-3), and the study was performed in compliance with the Declaration of Helsinki.

Cell culture. MCF-7 (ER$^+$/PR$^+$/HER2$^-$) breast cancer cells were obtained from ATCC (Manassas, VA, USA; HTB-22) and maintained in high glucose Dulbecco's modified Eagle's medium (DMEM Sigma-Aldrich, St. Louis, MO, USA) with 10% fetal bovine serum (FBS, Thermo Fisher Scientific, Waltham, MA, USA), 1% sodium pyruvate and penicillin/streptomycin (Sigma-Aldrich). The authenticity of MCF-7 cells was verified by STR DNA profiling (Eurofins Genomics GmbH, Vienna, Austria).

Non-transformed MCF-10A cells (ATCC; CRL-10317) were used within less than 10 passages. MCF-10A cells are routinely cultured in serum-free mammary epithelial basal medium (MEBM) supplemented with SingleQuot mammary growth additives (insulin, EGF, bovine pituitary extract, and hydrocortisone; Lonza, Slough, UK), where they retain a basal stem/progenitor cell phenotype [26].

Growth factor treatments. The supplements in MCF-10A culture comprise four individual components (insulin 5 μg/ml; human epidermal growth factor (hEGF) 20 ng/ml; hydrocortisone 0.5 μg/ml; bovine pituitary extract 0.2% (v/v)). To test the effect of each component, cells were grown in a medium that contained only three of the four supplements, and cells were assessed for p63 by immunohistochemistry after 24 h growth (i.e., MCF-10A cells were cultured in five different conditions, using complete medium or medium that lacked each individual growth factor but contained the other three growth factors at their standard concentrations). Based on the results obtained, MCF-7 cells were treated with insulin (5 μg/ml) or IGF-1 (100 ng/ml; Invitrogen, Thermo Fisher Scientific) added to their standard growth medium (DMEM containing 10% FBS). Unless indicated otherwise, cells were collected for analysis 24 h after the addition of the growth factor.

Immunohistochemistry. Sections (4 μm) of paraffin-embedded tumors were collected onto Superfrost Plus adhesive-coated microscope slides (Thermo Fisher Scientific) and dried overnight. Sections were dewaxed, rehydrated, and endogenous peroxidase was blocked in 3% hydrogen peroxide in PBS for 5 min. Antigen retrieval was performed by boiling in 1 mM EDTA, pH 8.0 for 20 min. After cooling, sections were blocked in antibody diluent (Dako, Agilent, Santa Clara, CA, USA) and immunostained using a mouse monoclonal antibody specific for ΔNp63 (clone ΔNp63-1.1), an affinity-purified rabbit antibody (ENN-47) specific for ΔNp63, and a mouse monoclonal antibody recognizing all p63 isoforms but not recognizing p73 or p53 (clone PAN-p63-6.1) [14, 27]. Sections stained without primary antibody served as the negative controls. See Table S1 for antibody details. Primary antibodies were applied overnight at 4°C and antibody binding was detected with Envision horseradish peroxidase (HRP)-polymer anti-mouse or anti-rabbit reagents (Dako) and 3,3‘-diaminobenzidine (DAB+, Dako) as the chromogen.

For immunostaining of cells cultured in the presence or absence of growth factors, cells were plated onto sterile glass slides and allowed to attach and grow for 24 h before treatment and were analyzed 24 h after treatment. After the culture medium was aspirated, cells were immediately fixed and permeabilized in methanol/acetone (50/50) at –20°C for 10 min and allowed to dry. Cells were blocked in 3% BSA in PBS followed by overnight incubation at 4°C with primary antibodies that recognize all p63 isoforms (mouse monoclonal 4A4 or PAN-p63-6.1), or are specific to ΔNp63 isoforms (affinity-purified rabbit serum ENN-47 or mouse monoclonal ΔNp63-1.1) [14, 27] (see Supplementary Table S1 for details of primary antibodies). After washing three times in PBS, staining was detected with Envision HRP-polymer reagents (Dako) or ABC Elite peroxidase (Vector Laboratories, Peterborough, UK) for rabbit or mouse primary

antibodies, using DAB as the chromogen. The omission of the primary antibody was used as the negative control.

All slides were counterstained with hematoxylin, dehydrated, cleared, mounted in resin, and viewed under bright field light microscopy. Positive cells were manually counted using at least 10 high-power fields for each experimental replicate, and experiments were performed at least three times.

Flow cytometry. Cells were trypsinized and single-cell suspensions were fixed in 4% buffered formaldehyde for 15 min at room temperature, permeabilized with 0.1% Triton X-100 in PBS for 5 min, blocked with 1% BSA in PBS, and incubated with p63 antibody (4A4; Dako) in blocking solution for 1 h at room temperature. After two washes in PBS, cells were incubated with DyLight488-conjugated goat anti-mouse IgG (Abcam, Cambridge, UK) for 1 h, washed in PBS, and resuspended in 500 µl PBS. Fluorescence was measured using a FACSVerse flow cytometer (BD Biosciences, Berks, UK).

Small molecule inhibitors of insulin/IGF signaling. To define which components of the insulin/IGF-1 signaling pathway are involved in ΔNp63 induction in MCF-7 cells, we used low molecular weight inhibitors of phosphoinositide 3 kinase (PI3K) (50 µM wortmannin; InvivoGen, Toulouse, France); mammalian target of rapamycin (mTOR) (10 µM rapamycin; Enzo Life Sciences, Farmingdale, NY, USA and 10 µM Ku-006379; BioVision, Milpitas, CA, USA); p38 MAP kinase (50 µM SB202190; Sigma-Aldrich); ERK1/2 (50 µM U0126; Tocris Bioscience, Bristol, UK), and a dual inhibitor of PI3K/mTOR kinases (10 µM BEZ235; SelleckChem, Houston, TX, USA). Cells were treated simultaneously with 100 ng/ml IGF-1 and inhibitor (or with an equal volume of solute as control) for 24 h before collection. Antibodies to phosphorylated target proteins (Supplementary Table S1) were used to assess the efficiency of these inhibitors on their target pathways.

Cells were also treated with the biguanide metformin (Sigma-Aldrich) that targets the AMPK/mTOR pathway. For these experiments, freshly plated cells were cultured overnight in low glucose (1 mg/ml) DMEM (Sigma-Aldrich) containing 10% FBS, 1% sodium pyruvate, sodium bicarbonate, and penicillin/streptomycin. Cells were then exposed to 100 ng/ml IGF-1 with or without 2 mM metformin for 24 h in the same medium. We were also able to retrieve paraffin-embedded tissue blocks of a matched pair of mouse xenografts of MCF-7 tumors from a previous experiment in which one mouse received sucrose solution in their drinking water and the other received phenformin in sucrose solution [28]. Sections were stained for ΔNp63 and the numbers of positive cells were counted in at least 10 high-power magnification fields for each sample (see Supplementary Information for details).

siRNA inhibition of FOXO signaling. One million MCF-7 cells were resuspended in 100 µl 4 mM KCl, 10 mM $MgCl_2$, 120 mM NaH_2PO_4/Na_2HPO_4, 10 mM HEPES pH 7.2, containing 400 nM siRNA specific to *FOXO1* or *FOXO3A*, or non-specific control siRNA using ON-TARGETplus SMART pools (Catalog numbers L-003006-00-0005; L-003007-00-0005; D-001810-OX, respectively; Horizon Discovery, Perkin-Elmer, Cambridge, UK; the sequences of these proprietary siRNAs are not provided by the supplier). Cells were transfected using electroporation (Amaxa Nucleofector II, Lonza, Basel, Switzerland) and allowed to grow for 24 h before IGF-1 addition, and were cultured for an additional 24 h before collection. Western blotting with FOXO antibodies (Supplementary Table S1) was used to assess the efficacy of the siRNAs on their targets.

Western blotting. Cells were lysed in NET buffer (150 mM NaCl, 1% NP-40, 50 mM Tris-HCl pH 8.0, 50 mM NaF, 5 mM EDTA, pH 8.0) supplemented with protease and phosphatase inhibitor cocktails (Sigma-Aldrich). Protein concentrations were measured by Bradford assay (Bio-Rad Laboratories, Watford, UK) and equal amounts of protein were separated by SDS-PAGE and blotted onto nitrocellulose. Membranes were blocked in 5% non-fat milk in PBS containing 0.1% Tween-20 (PBST) and incubated overnight at 4°C with primary antibodies diluted in a blocking solution. Following the supplier's recommendation, 5% BSA in TBST was used for blocking and antibody dilution for the detection of p-ERK1/2. Membranes were washed in PBST and PBS and incubated with HRP-conjugated swine anti-rabbit or rabbit anti-mouse (Dako) secondary antibodies for 1 h at room temperature. After further washes, blots were developed using enhanced chemiluminescence (ECL, Amersham Pharmacia Biotech, Bucks. UK), quantified using Fiji [29], and normalized to loading controls in the same sample (see Supplementary Table S1 for antibody details).

Reverse-transcription and quantitative PCR (RT-qPCR). Total RNA was isolated using RNeasy (Qiagen, Manchester, UK) or TRIzol (Invitrogen) and converted into cDNA using random primers and RevertAid H Minus Reverse Transcriptase (Thermo Fisher Scientific). SYBR Green MasterMix (Roche, Basel, Switzerland) was used for amplification and quantification in an ABI 7900HT Fast Real-Time PCR System (Thermo Fisher Scientific). RT-qPCR was performed in technical triplicates and the experiments were repeated twice to provide three biological replicates. Relative quantification of mRNA was determined based on $2^{-\Delta\Delta CT}$ using *ACTB* (β-actin) or *GAPDH* as a control. Primers were obtained from Generi Biotech (Hradec Kralove, Czech Republic; Supplementary Table S2) or as QuantiTect Primer Assay (Qiagen, Hilden, Germany) for *GAPDH*.

Statistical tests. Statistical tests were performed using VassarStats (https://VassarStats.net/). After confirming the normality of data distributions using Shapiro-Wilk tests, unpaired 2-tailed t-tests were employed for comparing cell line immunostaining, FACS, and RT-qPCR data. Mann-Whitney U test was used to analyze xenograft data due to the uneven and non-random distribution of ΔNp63 staining *in vivo*. Data are presented as mean ± SEM.

Results

ΔNp63 is present in a small subpopulation of tumor cells adjacent to the stroma in ER+ breast cancer metastases. ΔNp63 is known to be highly expressed in the basal (BL2) subtype of triple-negative breast cancer, where p63$^+$ cells generally constitute a high percentage (10–80%) of the tumor cell population and show a random distribution of positive cells throughout the tumor [7, 10–12]. Previous studies have shown the presence of ΔNp63$^+$ tumor cells in a proportion of human luminal breast cancers, where these cells represent basal-like breast CSCs (positive for CD44 or CD271; negative

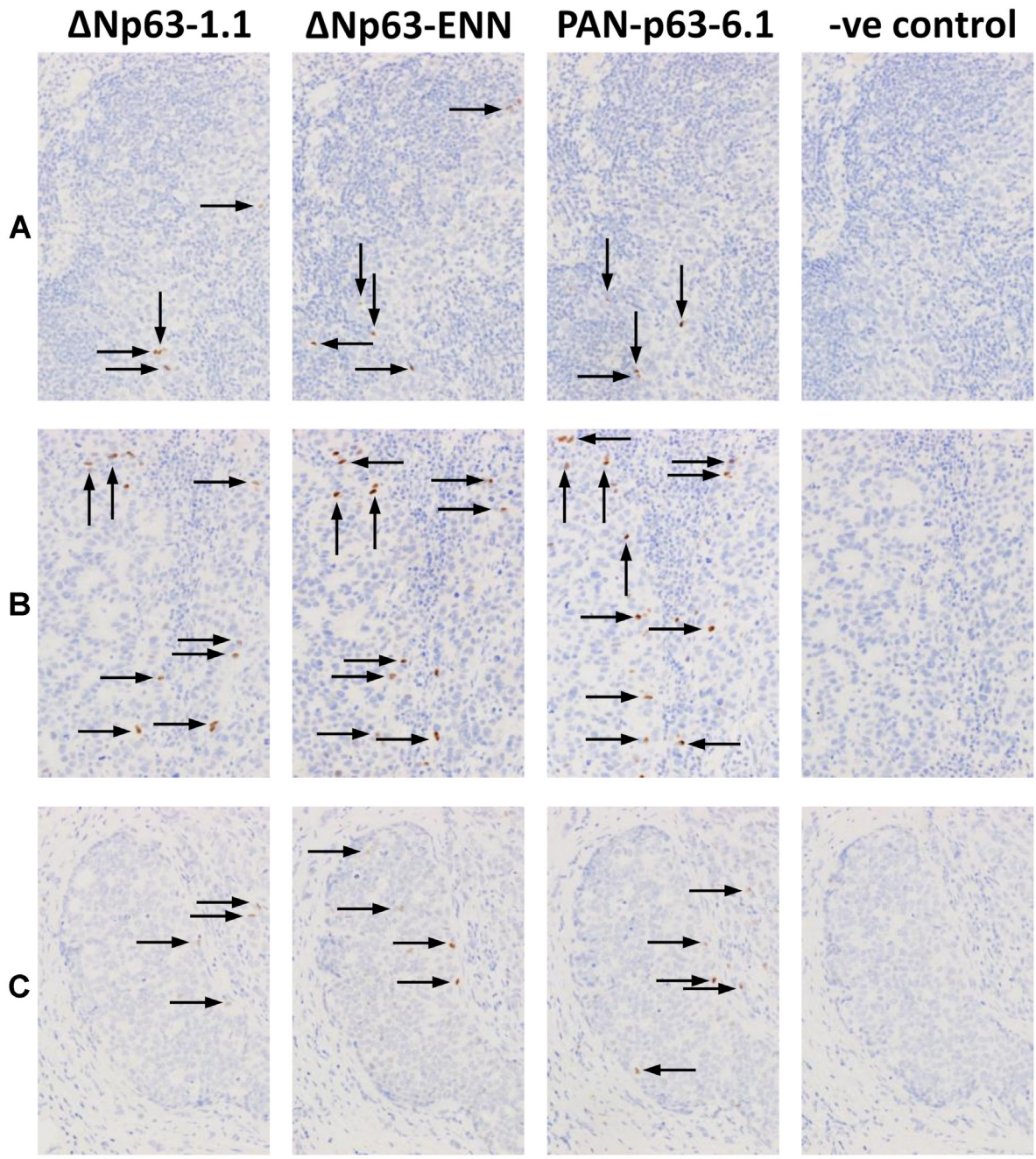

Figure 1. ΔNp63 is present in a population of metastatic breast cancer cells adjacent to the tumor stroma. A–C) Examples of lymph node metastases of primary human luminal-type (ER$^+$/HER2$^-$) breast cancers from three different patients. Consecutive sections were stained using two different antibodies specific for ΔNp63 (ΔNp63-1.1 and ENN-47), and an antibody for total p63 (PAN-p63-6.1). A negative control section where the primary antibody was omitted is also shown. Positive staining is seen as a brown color in the nucleus, and nuclei are counterstained blue with hematoxylin. Examples of p63$^+$ cells are indicated by arrows.

for ER and EMA or milk mucin) [17, 18]. Because ΔNp63 is expressed in normal basal/myoepithelial cells that may be present as a discontinuous layer surrounding the edges of primary breast cancers [3, 30], we initially confirmed the presence of ΔNp63$^+$ cells in local lymph node metastatic deposits, in which contaminating non-malignant basal cells will not be present. Immunohistochemistry from 28 patients with ER$^+$/HER2$^-$ breast cancer showed a small population of ΔNp63$^+$ cells in eight (29%) cases (Figures 1A–1C). These results confirm and extend previous observations of ΔNp63$^+$ cells [18] and CD271$^+$/ΔNp63$^+$ cells [17] in luminal breast cancer. Combining the current results with data from the previous reports shows that the incidence of ΔNp63$^+$ cells in ER$^+$/HER2$^-$ breast cancer metastasis is 39% (32 of 81 samples contain a subpopulation of ΔNp63$^+$ cells, see Supplementary Table S3 for details and statistical analysis). Notably, ΔNp63$^+$ basal-like breast CSCs commonly show a distinct location at the edge of tumor cell islands adjacent to the tissue stroma (Figures 1A–1C), suggesting that paracrine effects of the tumor microenvironment may be involved.

Insulin regulates ΔNp63 in basal mammary cells and luminal-type breast cancer cells. When grown as monolayers in their standard growth conditions, non-transformed MCF-10A cells are bi-potential progenitor basal mammary epithelial cells that express high levels of ΔNp63α [26, 31], and MCF-7 cells are an ER$^+$/PR$^+$/HER2$^-$ luminal A breast adenocarcinoma cell line with very low ΔNp63 levels [17, 18, 20, 21]. Immunohistochemistry using isoform-specific ΔNp63 antibodies showed that 4% of MCF-7 cells were p63$^+$, compared to more than 50% of MCF-10A cells in their standard growth medium (Figure 2A). We previously reported that growing MCF-7 cells as mammospheres in suspension culture (which selects for CSCs) increased the number of ΔNp63$^+$ cells [18]. Since the culture medium used for mammosphere production is similar to that of the MCF-10A culture medium (serum-free medium containing the same exogenous growth factors), we tested whether any of these additives are responsible for the different levels of ΔNp63 in MCF-7 and MCF-10A cells in monolayer culture. MCF-10A cells grown in medium lacking insulin showed a more than 3-fold reduction in the percentage of ΔNp63$^+$ cells (mean = 55.52% of 2,833 cells scored in the control vs. 17.54% of 3,149 cells without insulin; $p<0.001$), whereas removing other SingleQuot constituents did not affect the percentage of ΔNp63$^+$ MCF-10A cells. Conversely, adding insulin at the same concentration to MCF-7 cells increased the proportion of ΔNp63$^+$ cells by more than 6-fold (mean = 3.94% of 3,533 cells counted in control MCF-7 vs. 25.10% of 1,913 cells after insulin addition; $p<0.001$) (Figure 2B).

RT-qPCR showed that *ΔNp63* and *p63α* mRNAs are the predominant isoforms in both MCF-7 and MCF-10A cells, as previously reported [18, 21, 31]. In agreement with immunostaining data, MCF-10A cells had higher levels of *ΔNp63* and *p63α* mRNAs than MCF-7 under their recommended culture media (Supplementary Figure S1). The absence of insulin from MCF-10A culture medium decreased *ΔNp63* and *p63α* mRNAs to 33% to 40% of their original levels ($p<0.05$ for *ΔNp63* and $p<0.001$ for *p63α*). In contrast, adding insulin to MCF-7 cells increased these mRNAs by 4 to 5-fold ($p<0.01$ for *ΔNp63*) (Figure 2C).

IGF-1 regulates ΔNp63 in MCF-7 cells. The level of insulin used to culture MCF-10A cells stimulates both the insulin receptor and the IGF receptors [32]. Therefore, we tested whether IGF-1 also regulates ΔNp63 in a similar manner. Western blotting and RT-qPCR showed that IGF-1 increased ΔNp63 protein and mRNA levels in MCF-7 cells after 24 h (Figures 3A, 3B). Flow cytometry also indicated a more than 3-fold increase in the number of p63$^+$ MCF-7 cells after 24 h treatment with IGF-1 ($p<0.001$) (Figures 3C, 3D). Time course experiments showed that the rise in ΔNp63 levels was first visible within 4 h of IGF-1 treatment and continued to increase up to 24 h (Figure 3E).

Upregulation of ΔNp63 by IGF-1 requires PI3K/MAPK activity. Inhibitors of IGF-1-regulated pathways were used to identify the signaling cascade(s) involved in ΔNp63 induction in MCF-7 cells, with the effectiveness of inhibitors assessed by phospho-specific antibodies to the relevant targets. Wortmannin, an inhibitor of PI3K, blocked AKT activation and prevented ΔNp63 induction. Rapamycin, an inhibitor of mTORC1, reduced the levels of p-p70 S6K, as did the dual mTORC1/2 inhibitor Ku-006379, but these compounds did not reduce ΔNp63 following IGF-1 treatment. IGF-1 induction of ΔNp63 was prevented by SB202190 (p38 MAPK inhibitor) and U0126 (MEK1/2 inhibitor). The dual PI3K/mTOR inhibitor BEZ235 reduced both p-AKT and p-ERK1/2 and inhibited ΔNp63 protein induction by IGF-1 (Figure 4A). RT-qPCR demonstrated increased *ΔNp63* mRNA levels in MCF-7 cells after 24 h IGF-1 treatment, which was reduced to basal levels in the presence of wortmannin. Inhibition of p38 MAP kinase or ERK1/2 activity by SB202190 or U0126 also decreased *ΔNp63* mRNA to lower than basal levels in the presence of these inhibitors and IGF-1, whilst BEZ235 inhibited *ΔNp63* mRNA induction after IGF-1 by 50%, and rapamycin and Ku-006379 had no effect (Figure 4B).

FOXO and metformin/phenformin inhibit ΔNp63 induction by IGF-1. The FOXO family of transcription factors are key transcriptional regulators of insulin/IGF-1 signaling and are repressed by growth factor-mediated phosphorylation and cytoplasmic retention [33, 34]. FOXOs have been shown to regulate ΔNp63 transcription, with roles reported for FOXO1 in keratinocytes and for FOXO3a but not FOXO1 in breast and squamous cells [35, 36]. Using siRNAs to *FOXO1* or *FOXO3*, we showed that the siRNA pools were specific and effective at reducing their target proteins, FOXO1 or FOXO3a, with a higher level of knockdown achieved by *FOXO3* than *FOXO1* siRNA (Figure 5A, Supplementary Figures S2, S3). In our experiments, siRNAs to these FOXO members did not reduce ΔNp63 in IGF-1-treated MCF-7 cells but instead caused a 1.5-fold to 1.6-fold

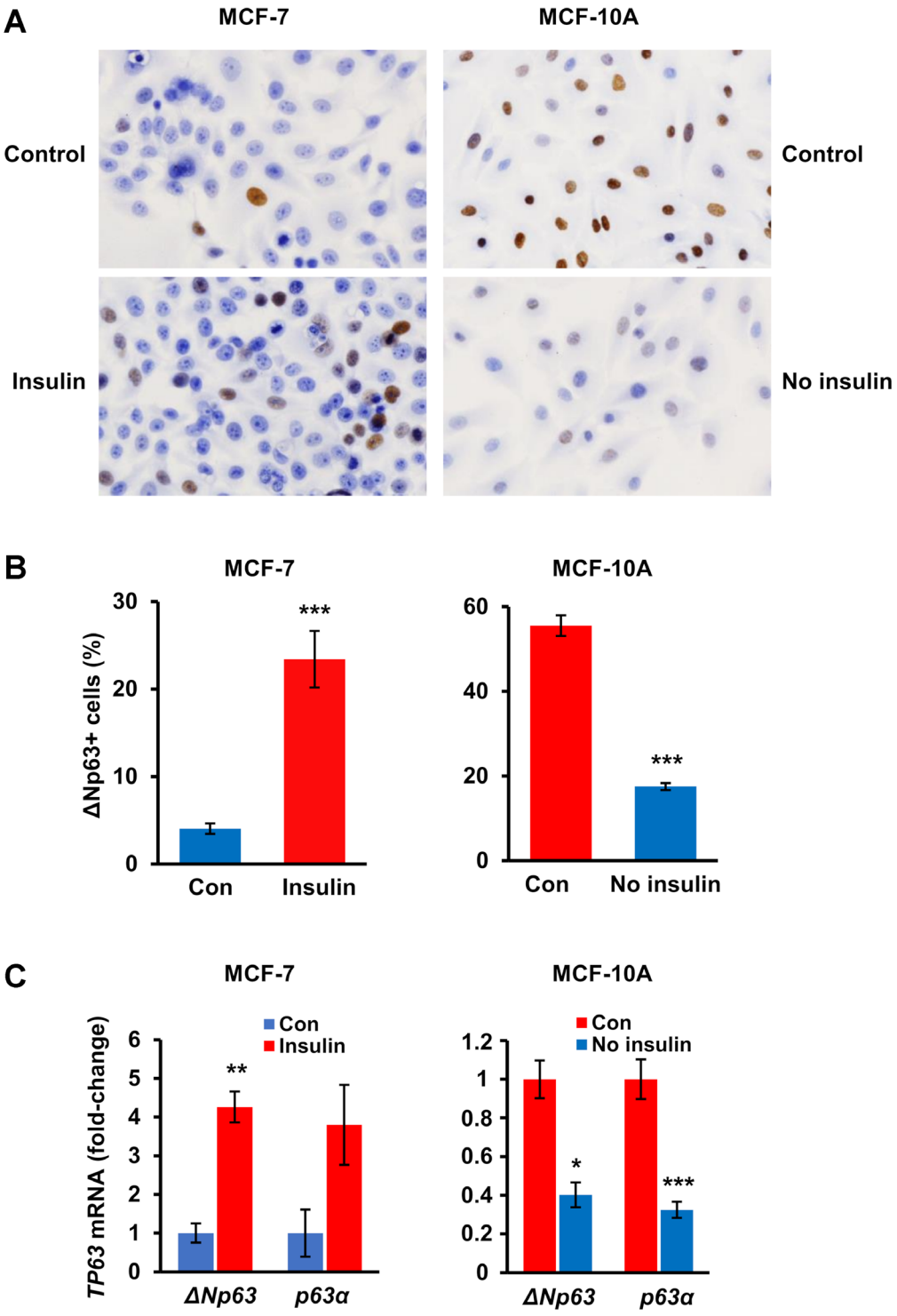

Figure 2. ΔNp63 protein and mRNA levels are regulated by insulin in non-transformed MCF-10A and transformed MCF-7 cells. A) Immunostaining for ΔNp63 in MCF-7 or MCF10-A cells cultured in the presence or absence of insulin in their growth medium. Positive staining is seen as a brown color and nuclei are stained blue with hematoxylin. B) Mean percentages of ΔNp63⁺ cells identified by immunohistochemistry and C) RT-qPCR of *TP63* mRNA (*ΔNp63* and *p63α* isoforms) in MCF-10A and MCF-7 cells. Cells were grown as monolayers in their standard growth conditions (Con) and in the absence of insulin (for MCF-10A) or in the presence of added insulin (for MCF-7 cells). Blue bars show cells grown in the absence of insulin and red bars show cells grown in the presence of insulin. mRNA data are shown as the fold-change in mRNA levels for *ΔNp63* and *p63α* normalized to *GAPDH* mRNA, with control cells set as a value of 1. Error bars show SEM (n = 3 biological replicates) *p<0.05, **p<0.01, ***p<0.001; t-test, control vs. test samples.

increase (Figure 5A). Since the insulin/IGF-1 pathway is intimately connected with cellular metabolism, we also investigated whether metformin influenced IGF-1 signaling to ΔNp63. For these experiments, MCF-7 cells were grown for 24 h in low-glucose medium. IGF-1 increased ΔNp63 protein and mRNA under these conditions, and the increases were reduced by metformin, with a larger effect seen on the protein level and a lower and non-statistically significant fall in mRNA (Figures 5B, 5C). In a preliminary *in vivo* investigation using MCF-7 mouse xenografts available from a previous study [28], the similar biguanide molecule, phenformin, reduced the number of ΔNp63⁺ cells in the single matched xenograft available for study, suggesting an *in vivo* effect similar to the *in vitro* effect (Supplementary Figure S4). More experiments will be required to confirm and delineate the mechanism of this effect.

Discussion

The CSC hypothesis proposes that tumors contain mixed populations of malignant cells that exhibit varying degrees of differentiation, including cells with stem or progenitor cell properties. According to this theory, CSCs are responsible for maintaining tumor growth, promoting therapy resistance, and initiating metastasis [24, 37]. In breast cancer, different CSC markers identify distinct cell populations [17, 19, 38] and at least two separate CSC subtypes exist, in which p63/CD271 or CD44 are markers of the basal subtype, and ALDH activity or milk mucin production are markers of the epithelial subtype [17, 18, 39]. It is also known that tumor cell phenotypes are not hard-wired, and phenotypic plasticity is an acknowledged feature of the CSC hypothesis, including the effects of the microenvironment [23–25, 39].

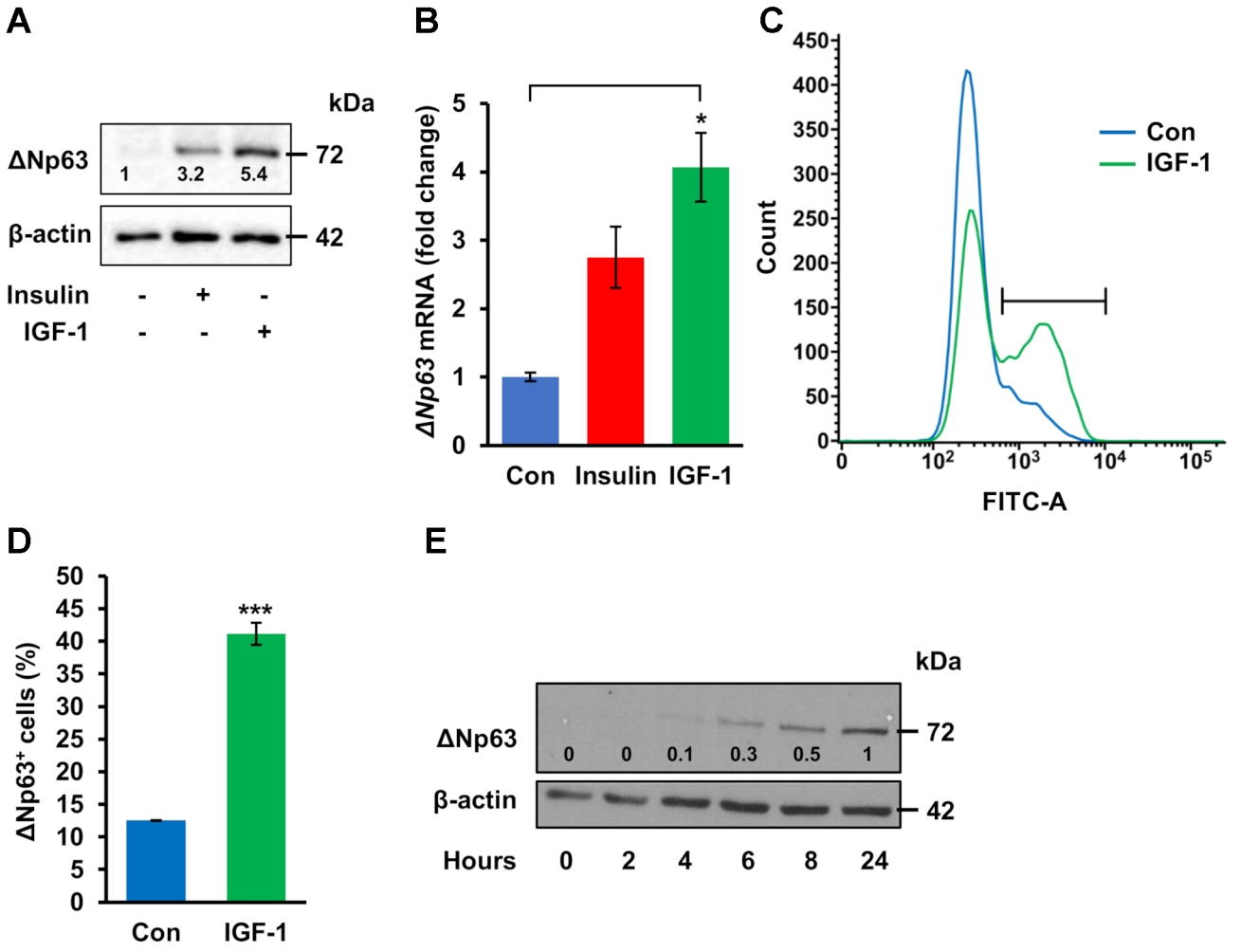

Figure 3. IGF-1 induces ΔNp63 in MCF-7 cells. A) Western blot of ΔNp63 protein and B) RT-qPCR of *ΔNp63* mRNA in MCF-7 cells treated with 5 μg/ml insulin or 100 ng/ml IGF-1 for 24 h. Control cells (Con) were grown in the same medium without additional growth factors (*p<0.05). Relative ΔNp63 protein and mRNA levels were normalized against β-actin. C) Representative flow cytometry of MCF-7 cells grown under standard conditions or in the presence of 100 ng/ml IGF-1. D) Mean percentages of ΔNp63⁺ cells derived from flow cytometry (*p<0.001). E) Western blotting of ΔNp63 in MCF-7 cells exposed to 100 ng/ml IGF-1 for the indicated times. β-actin served as a loading control. Numbers under the bands in western blots show the relative amount of ΔNp63 after normalization to the loading control and represent the mean values of replicate experiments.**

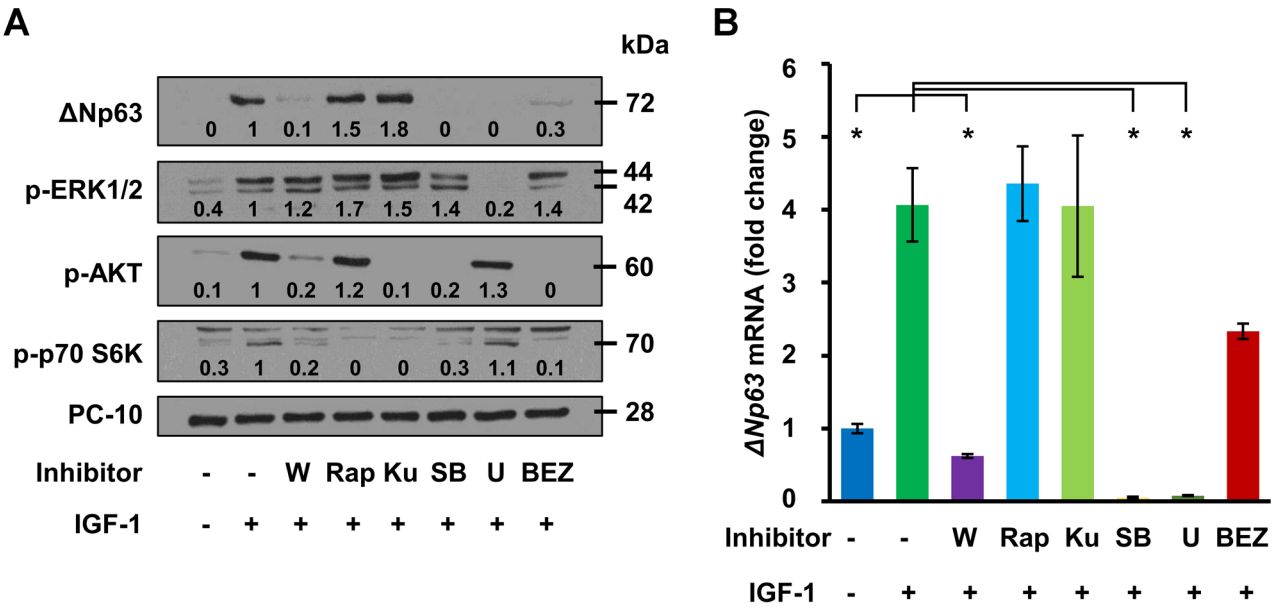

Figure 4. IGF-1 induction of ΔNp63 is dependent on PI3K and MAPK. A) Western blotting of control MCF-7 cells, cells treated with IGF-1, or cells treated with IGF-1 plus the indicated small molecule inhibitors. All cells were treated for 24 h. Numbers below bands refer to the relative levels of each protein normalized to PC-10 as a loading control, where IGF-1 treated cells without inhibitor are used as the comparator (value = 1.0) These numbers represent the mean of replicate experiments. Wortmannin (W), rapamycin (Rap), Ku-006379 (Ku), SB202190 (SB), U0126 (U), and BEZ235 (BEZ) were used as pathway inhibitors. Control blots for p-ERK1/2, p-AKT, p-p70 S6K as targets of the inhibitors are also shown. The addition of DMSO served as a negative control for inhibitors. Numbers under the bands in Western blots show the relative amount of ΔNp63 after normalization to the loading control and represent the mean values of replicate experiments. B) RT-qPCR for *ΔNp63* mRNA in MCF-7 cells treated as above (*p<0.05). p-ERK1/2, phosphorylated ERK1/2; p-AKT, phosphorylated AK strain transforming (also known as protein kinase B); p-p70 S6K, phosphorylated 70 kDa ribosomal protein S6 kinase.

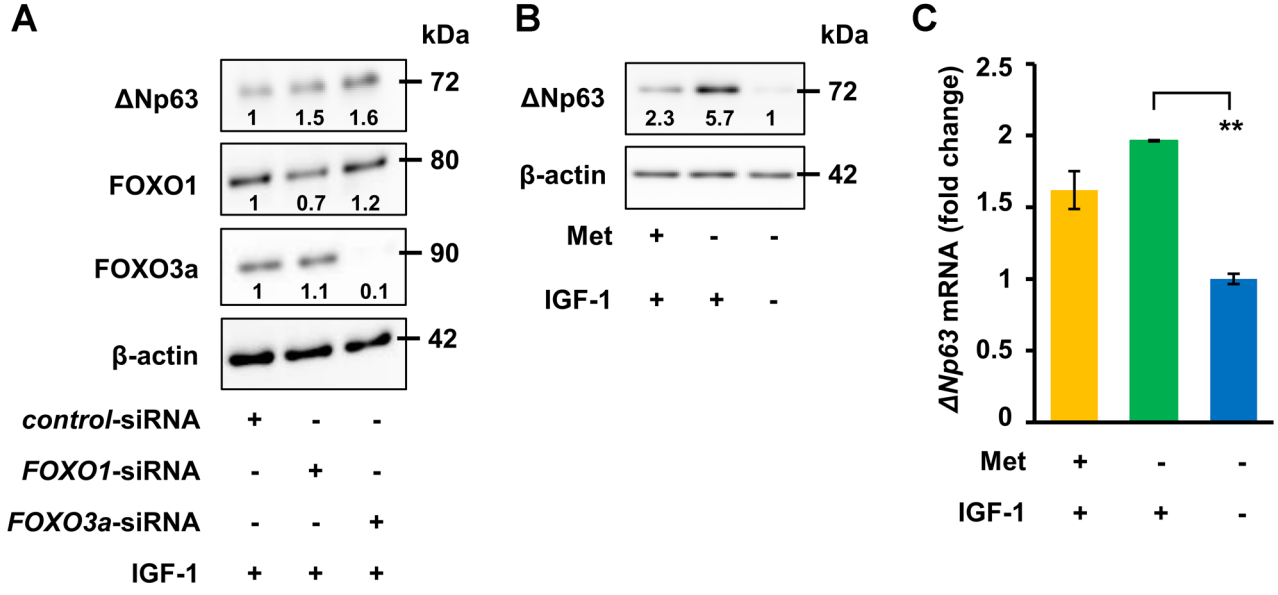

Figure 5. IGF-1 induction of ΔNp63 involves FOXO and is decreased by biguanides. A) Western blot of ΔNp63 in MCF-7 cells transfected with *control*, *FOXO1* or *FOXO3a* siRNAs. FOXO protein levels are shown to indicate the efficiency of siRNA-mediated target inhibition relative to control siRNA, and ΔNp63 and FOXO protein levels are normalized to β-actin. B) Western blot and C) RT-qPCR of ΔNp63 levels in MCF-7 cells cultured in low-glucose medium with or without IGF-1 and metformin (Met). Relative ΔNp63 protein and mRNA levels were normalized against β-actin and are shown as mean values from replicate experiments (p<0.01).**

Here, we investigated growth factors that potentially induce p63 in luminal ER$^+$ breast cancers, where p63 is known to directly impart CSC properties. The current and previous data [17, 18] indicate that ΔNp63$^+$ basal-like CSCs are present in about 40% of ER$^+$/HER2$^-$ breast cancers. These cells show a distinctive distribution at the tumor/stroma interface, which prompted us to investigate microenvironmental factors that may regulate ΔNp63. Using non-transformed MCF-10A mammary epithelial cells, which have high ΔNp63 levels under their normal growth conditions that maintain the undifferentiated bi-potential progenitor phenotype [18, 21, 31], we discovered that insulin is required to maintain ΔNp63 in these cells. Similarly, the addition of insulin to MCF-7 ER$^+$/HER2$^-$ luminal breast cancer cells increased ΔNp63 protein and mRNA levels, and IGF-1 caused a similar upregulation of ΔNp63. In particular, because IGF-1 is produced by breast fibroblasts present in the tumor stroma [40, 41], these findings implicate paracrine IGF signaling as one factor responsible for the upregulation of ΔNp63 in cells at the tumor/stroma interface. This notion is also in keeping with the effects of IGF signaling on promoting luminal progenitor and basal cell phenotypes in experimental breast cancers [42]. In addition to IGF, a variety of growth factors, cytokines, and cell adhesion molecules are all able to regulate ΔNp63 in cell-context-dependent manners (reviewed in [1, 2]), including IGF-1 or EGF induction of ΔNp63 in squamous epithelium [43–45]. On the other hand, Wnt signaling and STAT5 are reported to repress ΔNp63 in the mammary gland [5, 46], and p63 transcription is negatively regulated by methylation at the *TAp63* and/or *ΔNp63* gene promoters to silence transcription of each isoform independently in individual epithelial cell types [47, 48]. Similarly, epigenetic histone modifications at *ΔNp63* gene enhancers and binding of epigenome readers such as Brd4 determine transcription in a lineage-dependent manner in mammary epithelial cells [49, 50]. Thus, it is probable that insulin/IGF-1 is neither the sole regulator of ΔNp63 in mammary epithelium nor is it sufficient to induce ΔNp63 in luminal breast cancer cells in all situations.

We also investigated the biochemical mechanism involved in p63 regulation by insulin/IGF in breast cancer cells, to identify potential targets to intercept this pathway. Insulin/IGF-1 signaling may act through a PI3K-dependent pathway involving AKT and mTOR, and/or through Ras/MEK/ERK/MAPK or JAK/STAT pathways [51, 52]. We identified that IGF-1 induction of ΔNp63 in MCF-7 cells is dependent on PI3K and ERK/MAPK, in keeping with previous data that p38 MAPK regulates ΔNp63 in other cell types [53, 54]. Conversely, the observations that ΔNp63 regulates p38 MAPK and ERK signaling pathways [55, 56] imply the existence of complex self-regulatory feedback loops, a common finding in p63 regulation [2]. Insulin/IGF-1 and other growth factors that signal through PI3K/AKT/mTOR and MAPK/ERK negatively regulate the FOXO family of transcription factors by their phosphorylation and cytoplasmic retention, and the FOXO transcription factors play central roles in normal stem cells and in cancer but may show opposite effects depending on the cellular context [33, 34]. Thus, our findings that FOXO inhibition induces ΔNp63 are in keeping with increased ΔNp63 after growth factor treatment and the dependency of ΔNp63 on PI3K/mTOR signaling (current data and [43–45]). However, growth factor signaling has also been reported to decrease ΔNp63 in some situations through FOXO1 or FOXO3a [35, 50], which may relate to the cell-type specific functional effects of IGF-1 signaling on stem/progenitor cells in different breast cancer subtypes [57] and/or to the different duration and intensity of PI3K activation used in the different experimental settings (reviewed in [2]). Further studies of IGF dose and time course responses, and further delineation of FOXO effects will be required.

Finally, metformin has been shown to inhibit IGF-1 signaling in breast cancer, including inhibition of ERK1/2 activation [58, 59], and to downregulate ΔNp63 in squamous cell carcinoma cells [45]. We found that metformin inhibited IGF-1-mediated ΔNp63 induction in MCF-7 cells, further supporting the proposal that growth factor signaling pathways upregulate ΔNp63 in these luminal-type breast cancer cells. In these experiments, metformin decreased ΔNp63 protein levels to a higher extent than the mRNA levels, which is compatible with metformin acting to promote ΔNp63 protein ubiquitination and degradation in the proteasome [61]. Further experimental work will be required to delineate the precise mechanism by which metformin reduces ΔNp63 levels in mammary carcinoma cells. We also show preliminary data that the similar biguanide, phenformin, reduces ΔNp63 in MCF-7 xenografts *in vivo*. However, the effects of metformin in cancer patients are complex and involve modulation by metabolites produced by the stroma, as well as the direct effects on tumor cells [61, 62]. In addition, metformin added to standard therapeutic regimes prolongs invasive disease-free survival in HER2$^+$ breast cancer patients but not ER$^+$/HER2$^-$ patients [63], suggesting that metformin has a more prominent effect in breast cancers that rely on growth factor receptor activation as their main oncogenic process.

There are limitations to our study, including the use of single cell line examples of luminal-type breast cancer (MCF-7) and of non-malignant basal progenitor cells (MCF-10A). Although these are typical examples of these cell types, it will be important to verify the commonality of our results. The availability of additional xenografts and other models, including patient-derived xenografts and organoids, will also be useful to investigate the reliability of our findings for breast cancer patients, including HER2$^+$ and triple-negative cancers. Although we concentrated on the role of ΔNp63 due to its expression as the sole isoform in the cells studied, it will also be important to analyze additional p63 isoforms to investigate the precise variants

present, which may differ in different circumstances. Notwithstanding these limitations, our data clearly indicate a role for insulin/IGF as an important regulator of the breast basal CSC marker ΔNp63 in at least some clinically relevant situations.

In conclusion, we demonstrate that ΔNp63 is regulated by insulin/IGF-1 in both non-transformed mammary basal epithelial cells and MCF-7 luminal breast cancer cells, indicating IGF signaling as a potential regulator of intra-tumor phenotypic heterogeneity within luminal breast cancers. Dissection of the signaling components indicated a PI3K- and MAPK/ERK-dependent pathway involving FOXO repression, with relevance for therapeutic interference. Importantly, we also show that biguanides inhibit ΔNp63 induction by IGF, a finding that is likely to be involved in their clinical effects on the prophylaxis and treatment of human breast cancer.

Supplementary information is available in the online version of the paper.

Acknowledgments: This work was supported by the Czech Science Foundation (GACR 21-13188S), and the Ministry of Health, Czech Republic – conceptual development of research organization (MMCI, 00209805). MS received a Brno Ph.D. Talent Scholarship, funded by Brno City Municipality. BV acts as a consultant for Moravian Biotechnology, which supplied the isoform-specific p63 monoclonal antibodies used in this study. The company had no role in the study design or interpretation of the results, and was not involved in preparing or submitting the manuscript for publication. All other authors have no conflicts of interest to declare.

References

[1] FISHER ML, BALINTH S, MILLS AA. p63-related signaling at a glance. J Cell Sci 2020; 133: jcs228015. https://doi.org/10.1242/jcs.228015

[2] POKORNÁ Z, VYSLOUŽIL J, HRABAL V, VOJTĚŠEK B, COATES PJ. The foggy world(s) of p63 isoform regulation in normal cells and cancer. J Pathol 2021; 254: 454–473. https://doi.org/10.1002/path.5656

[3] BARBARESCHI M, PECCIARINI L, CANGI MG, MACRÌ E, RIZZO A et al. p63, a p53 homologue, is a selective nuclear marker of myoepithelial cells of the human breast. Am J Surg Pathol 2001; 25: 1054–1060. https://doi.org/10.1097/00000478-200108000-00010

[4] INMAN JL, ROBERTSON C, MOTT JD, BISSELL MJ. Mammary gland development: cell fate specification, stem cells and the microenvironment. Development 2015; 142: 1028–1042. https://doi.org/10.1242/dev.087643

[5] YALCIN-OZUYSAL O, FICHE M, GUITIERREZ M, WAGNER KU, RAFFOUL W et al. Antagonistic roles of Notch and p63 in controlling mammary epithelial cell fates. Cell Death Differ 2010; 17: 1600–1612. https://doi.org/10.1038/cdd.2010.37

[6] BALBONI AL, HUTCHINSON JA, DECASTRO AJ, CHERUKURI P, LIBY K et al. ΔNp63α-mediated activation of bone morphogenetic protein signaling governs stem cell activity and plasticity in normal and malignant mammary epithelial cells. Cancer Res 2013; 73: 1020–1030. https://doi.org/10.1158/0008-5472.CAN-12-2862

[7] CHAKRABARTI R, WEI Y, HWANG J, HANG X, BLANCO MA et al.: ΔNp63 promotes stem cell activity in mammary gland development and basal-like breast cancer by enhancing Fzd7 expression and Wnt signalling. Nat Cell Biol 2014; 16: 1004–1015. https://doi.org/10.1038/ncb3040

[8] MEMMI EM, SANARICO AG, GIACOBBE A, PESCHIAROLI A, FREZZA V et al.: p63 Sustains self-renewal of mammary cancer stem cells through regulation of Sonic Hedgehog signaling. Proc Natl Acad Sci U S A 2015; 112: 3499–3504. https://doi.org/10.1073/pnas.1500762112

[9] GATTI V, BONGIORNO-BORBONE L, FIERRO C, ANNICCHIARICO-PETRUZZELLI M, MELINO G et al. p63 at the Crossroads between Stemness and Metastasis in Breast Cancer. Int J Mol Sci 20: E2683, 2019. https://doi.org/10.3390/ijms20112683

[10] LEHMANN BD, BAUER JA, CHEN X, SANDERS ME, CHAKRAVARTHY AB et al. Identification of human triple-negative breast cancer subtypes and preclinical models for selection of targeted therapies. J Clin Invest2011; 121: 2750–2767.

[11] MATOS I, DUFLOTH R, ALVARENGA M, ZEFERINO LC, SCHMITT F. p63, cytokeratin 5, and P-cadherin: three molecular markers to distinguish basal phenotype in breast carcinomas. Virchows Arch 2005; 447: 688–694, 2005. https://doi.org/10.1007/s00428-005-0010-7

[12] COATES PJ, NENUTIL R, HOLCAKOVA J, NEKULOVA M, PODHOREC J et al. p63 isoforms in triple-negative breast cancer: ΔNp63 associates with the basal phenotype whereas TAp63 associates with androgen receptor, lack of BRCA mutation, PTEN and improved survival. Virchows Arch 2018; 472: 351–359. https://doi.org/10.1007/s00428-018-2324-2

[13] NEKULOVA M, HOLCAKOVA J, GU X, HRABAL V, GALTSIDIS S et al. ΔNp63α expression induces loss of cell adhesion in triple-negative breast cancer cells. BMC Cancer 2016; 16: 782. https://doi.org/10.1186/s12885-016-2808-x

[14] ORZOL P, NEKULOVA M, HOLCAKOVA J, MULLER P, VOJTESEK B et al. ΔNp63 regulates cell proliferation, differentiation, adhesion, and migration in the BL2 subtype of basal-like breast cancer. Tumour Biol 2016; 37: 10133–10140. https://doi.org/10.1007/s13277-016-5055-5

[15] HOLCAKOVA J, NEKULOVA M, ORZOL P, NENUTIL R, PODHOREC J et al. ΔNp63 activates EGFR signaling to induce loss of adhesion in triple-negative basal-like breast cancer cells. Breast Cancer Res Treat 2017; 163: 475–484. https://doi.org/10.1007/s10549-017-4216-6

[16] KUMAR S, WILKES DW, SAMUEL N, BLANCO MA, NAYAK A et al. ΔNp63-driven recruitment of myeloid-derived suppressor cells promotes metastasis in triple-negative breast cancer. J Clin Invest 2018; 128: 5095–5109. https://doi.org/10.1172/JCI99673

[17] KIM J, VILLADSEN R, SØRLIE T, FOGH L, GRØNLUND SZ et al. Tumor initiating but differentiated luminal-like breast cancer cells are highly invasive in the absence of basal-like activity. Proc Natl Acad Sci U S A 2012; 109: 6124–6129. https://doi.org/10.1073/pnas.1203203109

[18] LIU Y, NEKULOVA M, NENUTIL R, HORAKOVA I, APPLEYARD MV et al. ΔNp63/p40 correlates with the location and phenotype of basal/mesenchymal cancer stem-like cells in human ER+ and HER2+ breast cancers. J Pathol Clin Res 2020; 6: 83–93. https://doi.org/10.1002/cjp2.149

[19] LIU S, CONG Y, WANG D, SUN Y, DENG L et al. Breast cancer stem cells transition between epithelial and mesenchymal states reflective of their normal counterparts. Stem Cell Reports 2014; 2: 78–91. https://doi.org/10.1016/j.stemcr.2013.11.009

[20] DU Z, LI J, WANG L, BIAN C, WANG Q et al. Overexpression of ΔNp63α induces a stem cell phenotype in MCF7 breast carcinoma cell line through the Notch pathway. Cancer Sci 2010; 101: 2417–2424. https://doi.org/10.1111/j.1349-7006.2010.01700.x

[21] AMIN R, MORITA-FUJIMURA Y, TAWARAYAMA H, SEMBA K, CHIBA N et al. ΔNp63α induces quiescence and downregulates the BRCA1 pathway in estrogen receptor-positive luminal breast cancer cell line MCF7 but not in other breast cancer cell lines. Mol Oncol 2016` 10: 575–593. https://doi.org/10.1016/j.molonc.2015.11.009

[22] FISHER ML, BALINTH S, MILLS AA. ΔNp63α in cancer: importance and therapeutic opportunities. Trends Cell Biol 2023; 33: 280–292. https://doi.org/10.1016/j.tcb.2022.08.003

[23] OSHIMORI N, GUO Y, TANIGUCHI S. An emerging role for cellular crosstalk in the cancer stem cell niche. J Pathol 2021; 254: 384–394. https://doi.org/10.1002/path.5655

[24] BATLLE E, CLEVERS H. Cancer stem cells revisited. Nat Med 2017; 23: 1124–1134. https://doi.org/10.1038/nm.4409

[25] SHAN NL, SHIN Y, YANG G, FURMANSKI P, SUH N. Breast cancer stem cells: A review of their characteristics and the agents that affect them. Mol Carcinog 2021; 60: 73–100. https://doi.org/10.1002/mc.23277

[26] DEBNATH J, MUTHUSWAMY SK, BRUGGE JS. Morphogenesis and oncogenesis of MCF-10A mammary epithelial acini grown in three-dimensional basement membrane cultures. Methods 2003; 30: 256–268. https://doi.org/10.1016/s1046-2023(03)00032-x

[27] NEKULOVA M, HOLCAKOVA J, NENUTIL R, STRATMAN R, BOUCHALOVA P et al. Characterization of specific p63 and p63-N-terminal isoform antibodies and their application for immunohistochemistry. Virchows Arch 2013; 463: 415–425. https://doi.org/10.1007/s00428-013-1459-4

[28] APPLEYARD MVCL, MURRAY KE, COATES PJ, WULLSCHLEGER S, BRAY SE et al. Phenformin as prophylaxis and therapy in breast cancer xenografts. Br J Cancer 2012; 06: 1117–1122. https://doi.org/10.1038/bjc.2012.56

[29] SCHINDELIN J, ARGANDA-CARRERAS I, FRISE E, KAYNIG V, LONGAIR M et al. Fiji: an open-source platform for biological-image analysis. Nat Methods 2012; 9: 676–682. https://doi.org/10.1038/nmeth.2019

[30] LEE AHS. Use of immunohistochemistry in the diagnosis of problematic breast lesions. J Clin Pathol 2013; 6: 471–477. https://doi.org/10.1136/jclinpath-2012-201109

[31] CARROLL DK, CARROLL JS, LEONG CO, CHENG F, BROWN M et al. p63 regulates an adhesion programme and cell survival in epithelial cells. Nat Cell Biol 2006; 8: 551–561. https://doi.org/10.1038/ncb1420

[32] WORSTER DT, SCHMELZLE T, SOLIMINI NL, LIGHTCAP ES, MILLARD B et al. Akt and ERK control the proliferative response of mammary epithelial cells to the growth factors IGF-1 and EGF through the cell cycle inhibitor p57Kip2. Sci Signal 2012; 5: ra19. https://doi.org/10.1126/scisignal.2001986

[33] COOMANS DE BRACHÈNE A, DEMOULIN JB. FOXO transcription factors in cancer development and therapy. Cell Mol Life Sci 2016; 73: 1159–1172. https://doi.org/10.1007/s00018-015-2112-y

[34] HORNSVELD M, DANSEN TB, DERKSEN PW, BURGERING BMT. Re-evaluating the role of FOXOs in cancer. Semin Cancer Biol 2018; 50: 90–100. https://doi.org/10.1016/j.semcancer.2017.11.017

[35] GÜNSCHMANN C, STACHELSCHEID H, AKYÜZ MD, SCHMITZ A, MISSERO C et al. Insulin/IGF-1 controls epidermal morphogenesis via regulation of FoxO-mediated p63 inhibition. Dev Cell 2013; 26: 176–187. https://doi.org/10.1016/j.devcel.2013.05.017

[36] HU L, LIANG S, CHEN H, LV T, WU J et al. ΔNp63α is a common inhibitory target in oncogenic PI3K/Ras/Her2-induced cell motility and tumor metastasis. Proc Natl Acad Sci USA 2017; 114: E3964–E3973. https://doi.org/10.1073/pnas.1617816114

[37] CLARKE MF. Clinical and Therapeutic Implications of Cancer Stem Cells. N Engl J Med 2019; 380: 2237–2245. https://doi.org/10.1056/NEJMra1804280

[38] LIU Y, NENUTIL R, APPLEYARD MV, MURRAY K, BOYLAN M et al. Lack of correlation of stem cell markers in breast cancer stem cells. Br J Cancer 2014; 110: 2063–2071. https://doi.org/10.1038/bjc.2014.105

[39] COLACINO JA, AZIZI E, BROOKS MD, HAROUAKA R, FOULADDEL S et al. Heterogeneity of Human Breast Stem and Progenitor Cells as Revealed by Transcriptional Profiling. Stem Cell Reports 2018; 10: 1596–1609. https://doi.org/10.1016/j.stemcr.2018.03.001

[40] GUPTA PB, PASTUSHENKO I, SKIBINSKI A, BLANPAIN C, KUPERWASSER C. Phenotypic Plasticity: Driver of Cancer Initiation, Progression, and Therapy Resistance. Cell Stem Cell 2019; 24: 65–78. https://doi.org/10.1016/j.stem.2018.11.011

[41] RASMUSSEN AA, CULLEN KJ. Paracrine/autocrine regulation of breast cancer by the insulin-like growth factors. Breast Cancer Res Treat 1998; 47: 219–233. https://doi.org/10.1023/a:1005903000777

[42] KLEINBERG DL, BARCELLOS-HOFF MH. The pivotal role of insulin-like growth factor I in normal mammary development. Endocrinol Metab Clin North Am 2011; 40: 461–471. https://doi.org/10.1016/j.ecl.2011.06.001

[43] FARABAUGH SM, LITZENBURGER BC, ELANGOVAN A, PECAR G, WALHEIM L et al. IGF1R constitutive activation expands luminal progenitors and influences lineage differentiation during breast tumorigenesis. Dev Biol 2020; 63: 77–87. https://doi.org/10.1016/j.ydbio.2020.04.007

[44] BARBIERI CE, BARTON CE, PIETENPOL JA. Delta Np63 alpha expression is regulated by the phosphoinositide 3-kinase pathway. J Biol Chem 2003; 278: 51408–51414. https://doi.org/10.1074/jbc.M309943200

[45] MATHENY KE, BARBIERI CE, SNIEZEK JC, ARTEAGA CL, PIETENPOL JA. Inhibition of epidermal growth factor receptor signaling decreases p63 expression in head and neck squamous carcinoma cells. Laryngoscope 2003; 113: 936–939. https://doi.org/10.1097/00005537-200306000-00004

[46] POKORNA Z, VYSLOUZIL J, VOJTESEK B, COATES PJ. Identifying pathways regulating the oncogenic p53 family member ΔNp63 provides therapeutic avenues for squamous cell carcinoma. Cell Mol Biol Lett 2022; 27: 18. https://doi.org/10.1186/s11658-022-00323-x

[47] ASSEFNIA S, KANG K, GROENEVELD S, YAMAJI D, DABYDEEN S et al. Trp63 is regulated by STAT5 in mammary tissue and subject to differentiation in cancer. Endocr Relat Cancer 2014; 21: 443–457. https://doi.org/10.1530/ERC-14-0032

[48] POKORNA Z, HRABAL V, TICHY V, VOJTESEK B, COATES PJ. DNA Demethylation Switches Oncogenic ΔNp63 to Tumor Suppressive TAp63 in Squamous Cell Carcinoma. Front Oncol 2022; 12: 924354. https://doi.org/10.3389/fonc.2022.924354

[49] CAMPBELL JD, YAU C, BOWLBY R, LIU Y, BRENNAN K et al. Genomic, Pathway Network, and Immunologic Features Distinguishing Squamous Carcinomas. Cell Rep 2018; 23: 194–212.e6. https://doi.org/10.1016/j.celrep.2018.03.063

[50] PELLACANI D, BILENKY M, KANNAN N, HERAVI-MOUSSAVI A, KNAPP DJHF et al. Analysis of Normal Human Mammary Epigenomes Reveals Cell-Specific Active Enhancer States and Associated Transcription Factor Networks. Cell Rep 2016; 17: 2060–2074. https://doi.org/10.1016/j.celrep.2016.10.058

[51] NAGARAJAN S, BEDI U, BUDIDA A, HAMDAN FH, MISHRA VK et al. BRD4 promotes p63 and GRHL3 expression downstream of FOXO in mammary epithelial cells. Nucleic Acids Res 2017; 45: 3130–3145. https://doi.org/10.1093/nar/gkw1276

[52] SALTIEL AR. Insulin signaling in health and disease. J Clin Invest 2021; 131: 142241. https://doi.org/10.1172/JCI142241

[53] SIDDLE K. Signalling by insulin and IGF receptors: supporting acts and new players. J Mol Endocrinol 2011; 47: R1–10. https://doi.org/10.1530/JME-11-0022

[54] PAPOUTSAKI M, MORETTI F, LANZA M, MARINARI B, SARTORELLI V et al. A p38-dependent pathway regulates DeltaNp63 DNA binding to p53-dependent promoters in UV-induced apoptosis of keratinocytes. Oncogene 2005; 24: 6970–6975. https://doi.org/10.1038/sj.onc.1208835

[55] KANEKO Y, KOHNO T, KAKUKI T, TAKANO KI, OGASAWARA N et al.: The role of transcriptional factor p63 in regulation of epithelial barrier and ciliogenesis of human nasal epithelial cells. Sci Rep 2017; 7: 10935. https://doi.org/10.1038/s41598-017-11481-w

[56] BERGHOLZ J, ZHANG Y, WU J, MENG L, WALSH EM et al.: ΔNp63α regulates Erk signaling via MKP3 to inhibit cancer metastasis. Oncogene 2014; 33: 212–224. https://doi.org/10.1038/onc.2012.564

[57] WANG L, XIA W, CHEN H, XIAO ZX. ΔNp63α modulates phosphorylation of p38 MAP kinase in regulation of cell cycle progression and cell growth. Biochem Biophys Res Commun 2019; 509: 784–789. https://doi.org/10.1016/j.bbrc.2018.12.185

[58] FARABAUGH SM, BOONE DN, LEE AV. Role of IGF1R in Breast Cancer Subtypes, Stemness, and Lineage Differentiation. Front Endocrinol (Lausanne) 2015; 6: 59. https://doi.org/10.3389/fendo.2015.00059

[59] HADAD SM, COATES P, JORDAN LB, DOWLING RJO, CHANG MC et al. Evidence for biological effects of metformin in operable breast cancer: biomarker analysis in a pre-operative window of opportunity randomized trial. Breast Cancer Res Treat 2015; 150: 149–155. https://doi.org/10.1007/s10549-015-3307-5

[60] DOWLING RJO, NIRAULA S, CHANG MC, DONE SJ, ENNIS M et al. Changes in insulin receptor signaling underlie neoadjuvant metformin administration in breast cancer: a prospective window of opportunity neoadjuvant study. Breast Cancer Res 2015; 17: 32. https://doi.org/10.1186/s13058-015-0540-0

[61] YI Y, CHEN D, AO J, SUN S, WU M et al. Metformin Promotes AMP-activated Protein Kinase-independent Suppression of ΔNp63α Protein Expression and Inhibits Cancer Cell Viability. J Biol Chem 2017; 292: 5253–5261. https://doi.org/10.1074/jbc.M116.769141

[62] GUI DY, SULLIVAN LB, LUENGO A, HOSIOS AM, BUSH LN et al. Environment Dictates Dependence on Mitochondrial Complex I for NAD+ and Aspartate Production and Determines Cancer Cell Sensitivity to Metformin. Cell Metab 2016; 24: 716–727. https://doi.org/10.1016/j.cmet.2016.09.006

[63] ZHANG Z, LIANG X, FAN Y, GAO Z, BINDOFF LA et al. Fibroblasts rescue oral squamous cancer cell from metformin-induced apoptosis via alleviating metabolic disbalance and inhibiting AMPK pathway. Cell Cycle 2019; 18: 949–962. https://doi.org/10.1080/15384101.2019.1598727

[64] GOODWIN PJ, CHEN BE, GELMON KA, WHELAN TJ, ENNIS M et al. Effect of Metformin vs Placebo on Invasive Disease-Free Survival in Patients With Breast Cancer: The MA.32 Randomized Clinical Trial. JAMA 2022; 327: 1963–1973. https://doi.org/10.1001/jama.2022.6147

https://doi.org/10.4149/neo_2023_230719N376

ΔNp63 is regulated by insulin/IGF-1 signaling in normal basal/progenitor mammary cells and in luminal-type breast cancer cells

Michaela STENCKOVA[1,2], Yajing LIU[3], Marta NEKULOVA[1], Jitka HOLCAKOVA[1], Zuzana POKORNA[1], Rudolf NENUTIL[1], Alastair M. THOMPSON[4], Borivoj VOJTESEK[1,*], Philip John COATES[1,*]

Supplementary Information

MCF-7 xenografts. A matched pair of formalin-fixed paraffin-embedded MCF-7 xenograft tissues from mice treated with the biguanide phenformin or control untreated mice were available from a previous study [1]. Animal procedures had been carried out under project licenses No. 60/3405 and 60/3729 after local ethical review and according to the guidelines of the UKCCCR. In brief, female NU/NU nude mice with established xenografts had been provided with water containing 300 mg/kg phenformin and 5% sucrose for palatability, or with 5% sucrose water only. In accordance with the recommended UKCCCR procedure guidelines, animals were killed by exposure to rising concentrations of carbon dioxide (20% chamber volume displacement/minute), confirmed by lack of respiration and cardiac arrest. Xenograft tumors were excised, fixed in formalin and processed to paraffin wax. Due to previous use of these tissues, only a single treated and concurrent control tumor xenograft were available for study. Fresh sections of xenografts (4 μm) were collected onto adhesive slides and air-dried overnight. Sections were dewaxed and rehydrated before blocking endogenous peroxidase and antigen retrieval by boiling in 1mM EDTA for 20 min. After cooling and washing in PBS, sections were blocked in Dako blocking buffer before incubation in affinity purified rabbit anti-ΔNp63 antibody (ENN47) overnight and detection with HRP-polymer secondary reagents (Dako, Agilent, Santa Clara, California, USA). Sections were counterstained with hematoxylin, dehydrated and mounted in resin. Positive cells were counted in at least 10 independent high-power fields for each xenograft. Due to the uneven and non-random distribution of ΔNp63 staining *in vivo*, the Mann-Whitney U test was used for statistical analysis.

Reference

[1] APPLEYARD MVCL, MURRAY KE, COATES PJ, WULLSCHLEGER S, BRAY SE et al. Phenformin as prophylaxis and therapy in breast cancer xenografts. Br J Cancer 2012; 106: 1117–1122. https://doi.org/10.1038/bjc.2012.56

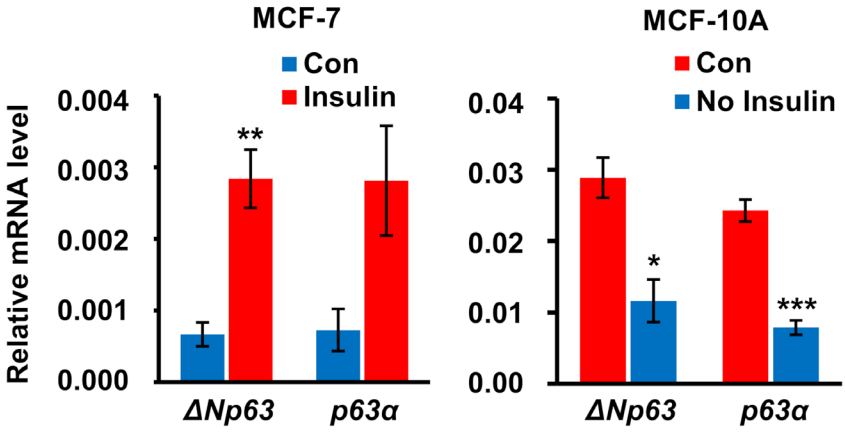

Supplementary Figure S1. RT-qPCR of p63 mRNA levels. The graphs show the mean levels of *TP63* mRNAs (*ΔNp63* and *p63α*) in MCF-7 and MCF-10A cells with (red bars) or without insulin (blue bars) in their culture medium. The *y* axis shows the mRNA level normalized to GAPDH, which is set at 1.0. Error bars represent sem. Note that the *y* axes have different scales reflecting the different levels of p63 in the two cell lines. *p<0.05; **p<0.01; ***p<0.001, two-tailed t-test.

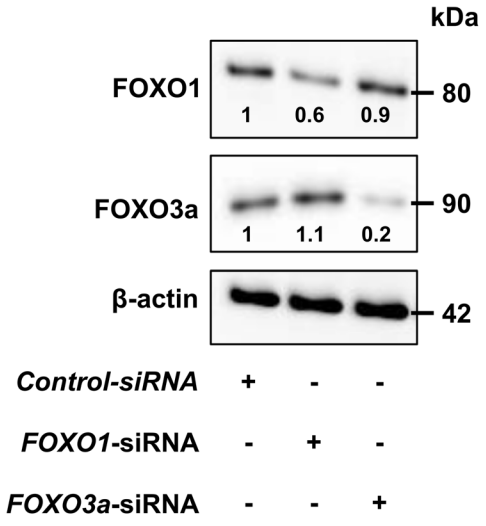

Supplementary Figure S2. Efficiency and specificity of *FOXO* siRNAs. MCF7 cells were transfected with *control* siRNA or siRNA pools targeting either *FOXO1* or *FOXO3a*. Western blotting for FOXO1 and FOXO3a was performed using cells collected 48 h after transfection. β-actin was used as loading control.

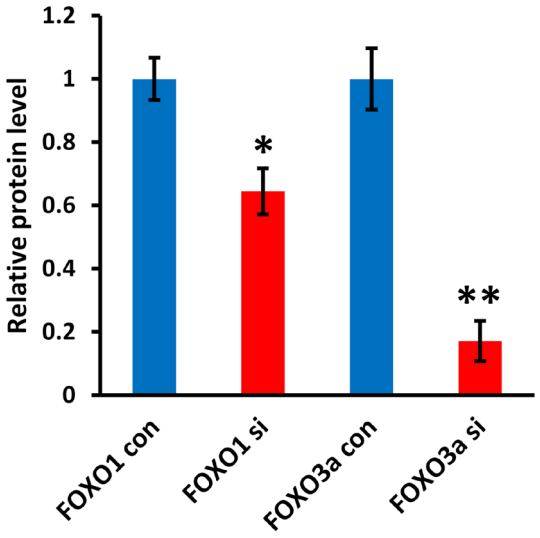

Supplementary Figure S3. Statistical analysis of *FOXO* siRNA effects on their targets. As in Figure 5, MCF7 cells were transfected with *control* siRNA, *FOXO1* siRNA, or *FOXO3a* siRNA, and then treated with IGF for 24 h. Densitometry was performed to measure the levels of FOXO proteins, normalized to β-actin. The levels of FOXO1 or FOXO3a in cells transfected with *control* siRNA are set to 1. Error bars represent SEM. *p=0.0235; **p=0.0034; two-tailed t-test (n=3).

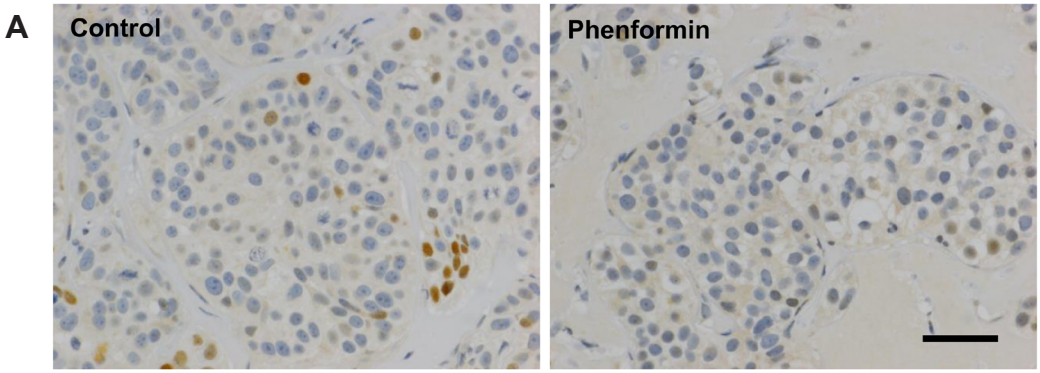

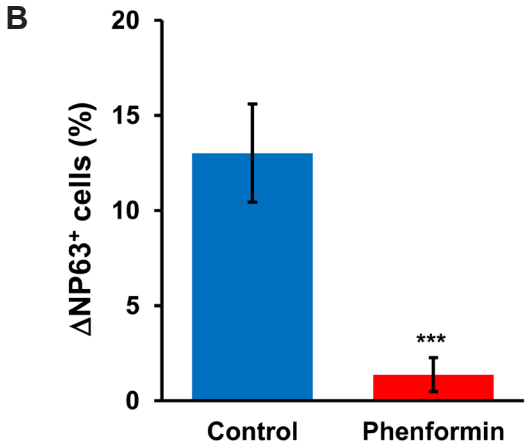

Supplementary Figure S4. ΔNp63 is reduced by biguanides in MCF-7 xenografts. A) Representative images of ΔNp63 immunohistochemical staining of MCF-7 xenografts from mice treated with phenformin (Phen) or untreated (Con). B) Quantitation of ΔNp63 immunohistochemistry on MCF-7 xenografts. ***p<0.001 (two-tailed Mann-Whitney U-test).

Supplementary Table S1. Primary antibodies.

Antigen	Species/type	Supplier[1]	Name
ΔNp63	Mouse monoclonal	In-house	ΔNp63-1.1
ΔNp63	Affinity purified rabbit polyclonal	In-house	ENN-47
p63	Mouse monoclonal	In-house	PAN-p63-6.1
FOXO1	Rabbit monoclonal	CST	C2DH4
FOXO3a	Rabbit monoclonal	CST	D19A7
p-AKT (Ser473)	Rabbit monoclonal	CST	736E11
p-ERK1/2	Rabbit monoclonal	CST	20G11
p-p70 S6K (Thr389)	Affinity purified rabbit polyclonal	CST	9205
β-actin[2]	Mouse monoclonal	SC	C4
PCNA[2]	Mouse monoclonal	In-house	PC10

[1]CST-Cell Signaling Technology, Danvers, MA, USA; SC-Santa Cruz Biotechnology, Dallas, TX, USA
[2]used as loading controls (please see https://blog.cellsignal.com/choosing-a-western-blot-loading-control-cst-blog; https://www.ptglab.com/news/blog/loading-control-antibodies-for-western-blotting/ ; https://www.abcam.com/products?keywords=loading%20controls&selected.classification=Primary +antibodies; https://www.sigmaaldrich.com/technical-documents/technical-article/protein-biology/western-blotting/loading-controls-western-blotting)

Supplementary Table S2. Primer sequences qPCR. Sequences are given 5'–3'.

Isoform	Forward primer	Reverse primer
ΔNp63	AGCCAGAAGAAAGGACAGCA	TCACTAAATTGAGTCTGGGCAT
TAp63	GTCCCAGAGCACACAGACAA	TAGCATGGACTGTATCCGCA
p63α	GAGGTTGGGCTGTTCATCAT	GAGGAGAATTCGTGGAGCTG
p63β	AACGCCCTCACTCCTACAAC	GCCAGATCCTGACAATGCTG
p63γ	GAAACGTACAGGCAACAGCA	GAAACGTACAGGCAACAGCA
ACTB	GCCGACAGGATGCAGAAGGAG	CTAGAAGCATTTGCGGTGGAC

Supplementary Table S3. Numbers of ER$^+$ breast cancer metastases containing (Positive) or not containing (Negative) a subpopulation of ΔNp63-positive cells. Data are taken from the current study and two previous studies.

References	Total	Positive	Negative	Percent positive
Kim et al 2012	32	17	15	53%
Liu et al 2020	22	7	15	32%
Current study	28	8	20	29%
Total	**82**	**32**	**50**	**39%**

p=0.11; Chi-square test

References

KIM J, VILLADSEN R, SØRLIE T, FOGH L, GRØNLUND SZ et al. Tumor initiating but differentiated luminal-like breast cancer cells are highly invasive in the absence of basal-like activity. Proc Natl Acad Sci U S A 2012; 109: 6124-6129. https://doi.org/10.1073/pnas.1203203109

LIU Y, NEKULOVA M, NENUTIL R, HORAKOVA I, APPLEYARD MV et al. ΔNp63/p40 correlates with the location and phenotype of basal/mesenchymal cancer stem-like cells in human ER+ and HER2+ breast cancers. J Pathol Clin Res 2020; 6: 83-93. https://doi.org/10.1002/cjp2.149